Natural Hazards
https://doi.org/10.1007/s11069-020-04012-w

ORIGINAL PAPER

Spatiotemporal relation of RADAR-derived land subsidence with groundwater and seismicity in Semnan—Iran

Hamidreza Koohbanani[1] · Mohammadreza Yazdani[1] · Sayyed Keivan Hosseini[2]

Received: 1 June 2019 / Accepted: 25 April 2020

Abstract
Due to excessive harvesting of underground water resources in many important aquifers inside Iran, ground subsidence is occurring at different speeds. In present study, InSAR processing was applied to identify land displacement by using Sentinel-1A. For this target, 17 frames of images during 2015–2019 with small temporal-perpendicular baseline were allocated and using SBAS approach were analyzed. After removing unnecessary noise and phases, phase shift due to land deformation is extracted and then converted to subsidence. Besides SAR images, fluctuations of groundwater were analyzed using piezometric data for last 10 years. Then the spatial pattern relationship between subsided regions and underground water resources as well as urbanization was investigated. Throughout this period, all datasets reveal 125 km^2 bowl subsidence in a maximum rate of 10 cm/year. Generally, areas with high rates of subsidence are located between the industrial town and city of Semnan over clay foundation with high rates of groundwater head decline. Moreover, surveying the piezometers and landuse change map obtained from Landsat indicates that due to the intense groundwater withdrawal as a result of industrialization and urbanization, the maximum annual decline of groundwater head at 123 cm/year is detected. Our preliminary investigation shows some spatiotemporal positive correlation between the subsidence and seismicity of the area. Considering the fragility of arid ecosystems and increasing the population of Semnan, it is recommended that the development of industries with high water consumption is prevented and the groundwater resources policies should seek to strictly reduce overusing of groundwater in agricultural lands and urban areas.

Keywords Interferometry · RADAR · Displacement · Groundwater · Hazard · Earthquake

1 Introduction

Subsidence is considered as one of the diverse forms of downward settling of the ground with minor horizontal movements, ranging from local to broad regional falling of ground level which is mostly irreversible (Antonellini et al. 2019). This is one of the most

✉ Mohammadreza Yazdani
m_yazdani@semnan.ac.ir

[1] Faculty of Desert Studies, University of Semnan, Semnan, Iran

[2] Earthquake Research Center, Ferdowsi University of Mashhad, Mashhad, Iran

Published online: 16 May 2020

significant negative environmental consequences of broad groundwater extraction, which primarily occurs in arid and semiarid environments (Foroughnia et al. 2019). In recent decades, rapid population growth combined with urban and industrial development have caused the increase in water needs in big cities (Haghshenas Haghighi and Motagh 2019). Subsidence is addressed by many scholars in many areas across the world such as Orihuela city in Spain (Tomas et al. 2010), Mexico city (Osmanoglu et al. 2011), Indonesia (Chaussard et al. 2013), Vancouver (Samsonov et al. 2014), Tehran (Pirouzi and Eslami 2017), Rafsanjan in Iran (Motagh et al. 2017), Saudi Arabia (Othman et al. 2018), California (Jeanne et al. 2018) and Beijing (Chen et al. 2018). Continuous extraction of groundwater has led to significant subsidence of plains, so that reports in some areas indicate that the subsidence rate has exceeded 20–30 cm/year (Davoodijam et al. 2015). Although the high relation between the land subsidence and the reducing water resources is mentioned by many experts (Declercq et al. 2017; Figueroa-Miranda et al. 2018) and many efforts have been made to fully understand this phenomenon, so far a comprehensive and accurate model prediction of the subsidence has not been provided. By declining the head of groundwater, an increase in effective stress caused by a decrease in pore water pressure (PWP) results in subsidence. In other words, reducing PWP and increasing the effective stress is prolonging; therefore, with following the reduction of the piezometric level, the subsidence will occur with a time delay (Angourani et al. 2014).

The subsidence due to volume reduction, by natural and/or anthropogenic factors, generally is a slow phenomenon occurring over relatively large areas (Othman et al. 2018). The subsidence due to the drop in fluid level mainly happens in unconsolidated sediments adjacent to the sand layers (Salehi et al. 2012). In these conditions, non-elastic density occurs due to the growth in effective stress in the soil and finally the sorting of the soil particles and the thickness of the vertical layer decreases (Bell 1999). The uneven drop in the groundwater level and the heterogeneity of the aquifer texture causes anomalous displacement. Consequently, the fissures and faults on the surface of the earth are observed (Haghighatmehr et al. 2011).

The cracks and slits of land surface spreading slowly and quietly. On the other hand, this phenomenon can lead to more abnormal results by altering the some hydrogeological characteristics, such as direction and speed of groundwater flow, underground water table, etc. (Holzer and Galloway 2005). The high rate of subsidence results in the destruction of structures such as buildings, roadways, bridges, transfer pipes and dams (Hoffmann 2005) and flooding (Rodolfo and Siringan 2006). In recent years, extensive efforts have been made to measure the changes in the earth's crust using technologies such as precise leveling (Bell et al. 2002) and borehole extensometric settlement (Tomas et al. 2005). Also, two recent technologies are GPS (Global Positioning System) and SAR (Synthetic Aperture Radar) which have been used to increase the accuracy of surface deformation to measurement. Both GPS systems with high temporal resolution and SAR processing with high spatial resolution are useful tools for estimation of small changes in land surface deformation.

Interferometry using InSAR (Interferometric Synthetic Aperture Radar) is a precise method based on the use of at least two SAR images from a specific location and is able to measure the changes in the line of sight of the satellite accurately at large scale over different time intervals with measuring precision at millimeters (Tung et al. 2016). This method is also used to estimate displacements on a large scale. The basis of InSAR method is simple. If two SAR images of a region are taken at two different times, the interferogram for the combination of these two phase images will show slight changes in the Earth's surface on a millimeter scale. SAR imagery is produced by reflecting radar signals off a target area and measuring the two-way travel time back to the satellite (Jeanne et al. 2018). The phase

shift of two SAR images signifies the displacement of the surface. The amount of motion is corresponding to half the wavelength (Vajedian et al. 2010). So, Interferometric Synthetic Aperture Radar (InSAR) is a powerful satellite-based technique for measuring the land deformation (Huang et al. 2017). In recent years in order to measure the displacement of the Earth's surface, the InSAR method has been considered as one of the space-geodetic methods (Zerbini et al. 2007). For example, Dehghani (2016), through this method and Envisat images, assessed subsidence in the Mashhad plain during the 2003 to 2005. The results of her study showed that the subsidence of Mashhad plain in most cases was 23 cm per year. She also found the piezometric level drop is related with the Earth's surface displacement. However, in some wells, despite the decrease in the piezometric level, the subsidence signal was not observed.

The present research is one of the first studies in Iran to use the capabilities of the Sentinel radar images of the ESA (European Space Agency), which aims to measure the magnitude and extent of the subsidence event using radar interferometry technology. The Sentinel-1A images have been developed by the ESA, and its imaging has begun since the 14th of January 2014. The operational lifespan is considered 7 years. The satellite was a Sun-synchronous orbit with an orbital height of 693 km and is shooting in a C band with a wavelength of 55.5 mm and a resolution of 12 days (Ouyang et al. 2019). One of the products of Sentinel-1A is the SLC data, with a resolution of 20×5 m and is able to estimate the displacement with accurately in millimeters for interferometry studies (Rucci et al. 2012). In this study, we argue and assess surface displacement and agents that have contributed to the formation and expansion of subsidence in Semnan city.

2 Materials and methods

2.1 Study area

Semnan plain is located in the 53° 30′ to 53° 35′ eastern longitude and 35° 22′ to 35° 29′ the northern latitude with area of 703 km^2. Semnan is capital of Semnan province and situated in central Iran. This area has a semiarid climate. Due to its proximity to Tehran and the special geographical location, Semnan has a growing economic and industrial prospects. In the past two decades, rapid industrial and agricultural development in this region, coupled with rapid population growth and consequently an increase in water demand, has led to an increase in harvesting of groundwater. The mean annual precipitation is less than 140 mm (Hejazizadeh et al. 2015) (Fig. 1).

3 Research methodology

The Sentinel-1A sensor is routinely sensing land over Iran with minimum orbit repeat cycle of 6 days since 2014 at both descending and ascending modes. Specifically, all the accessible images from 2014 to 2019 at path 137 and frame 474 have been considered for our research. A total of 90 acquisitions, taken every 12 days at descending geometry, have been considered. These Single Look Complex (SLC) data with VV polarization, available from ESA data hub in the Interferometric Wide (IW) swath mode, have pixel spacing of about 20 m by 5 m (azimuth and range components, respectively). The incidence angle of center scene is about 34°. In general, shorter temporal baseline provides more coherent

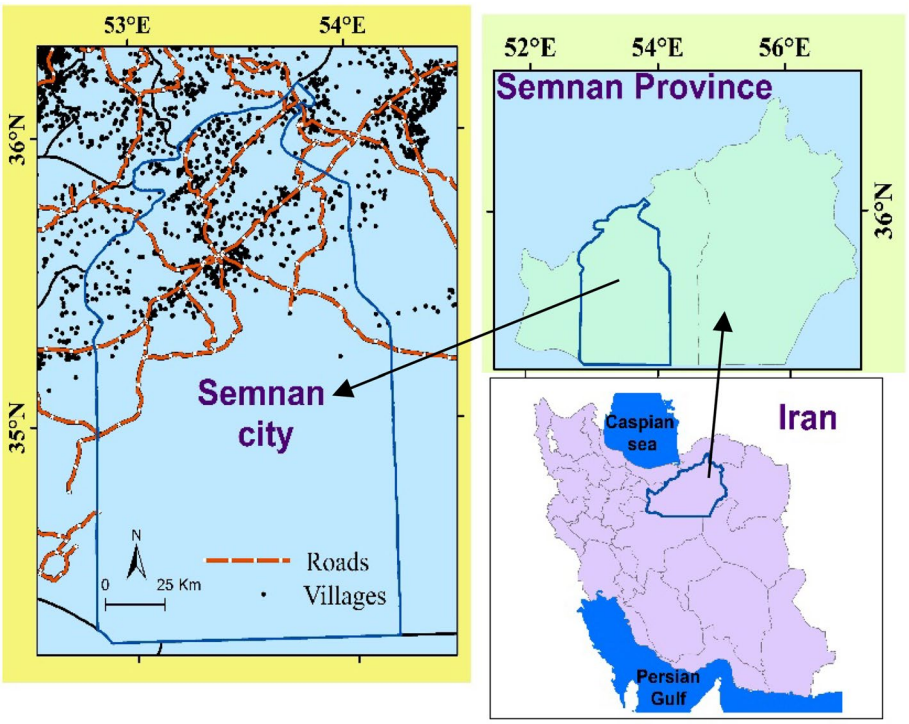

Fig. 1 Geographical location of Semnan in Iran

interferometric phases (Marbouti et al. 2017). For this goal and to reducing the size of dataset, the 17-m perpendicular baseline threshold value was applied to the whole Sentinel-1A archive. Finally, 17 images were selected with the allocated perpendicular baseline (Fig. 2 and Table 1). In present research, we followed short temporal baseline approach (SBAS) for InSAR time series evaluation. In SBAS method, each interferogram contains

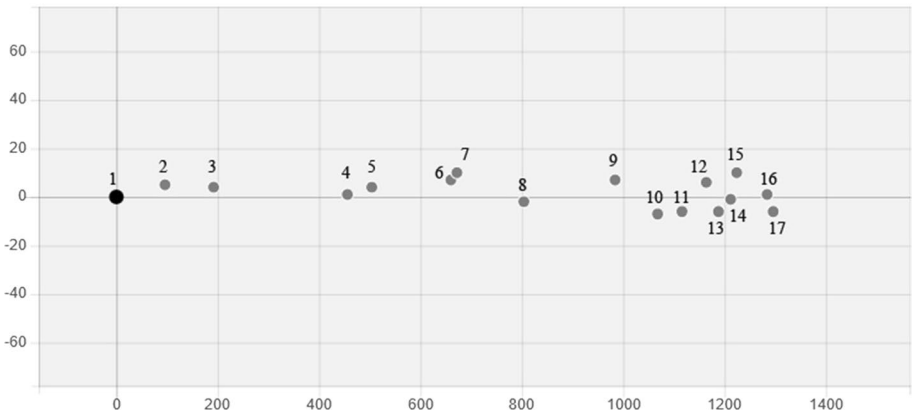

Fig. 2 Temporal (*x*-axis) and perpendicular (*y*-axis) baseline of the Sentinel-1 acquisitions

Table 1 Sentinel acquisitions dates (the number of images is as shown in Fig. 2)

1	2015-06-24	2	2015-09-28	3	2016-01-02	4	2016-09-22
5	2016-11-09	6	2017-04-14	7	2017-04-26	8	2017-09-05
9	2018-03-04	10	2018-05-27	11	2018-07-14	12	2018-08-31
13	2018-09-24	14	2018-10-18	15	2018-10-30	16	2018-12-29
17	2019-01-10						

the rate of surface changes between two acquisition dates. In order to obtain a time series analysis of the field displacement, phase information from all interferograms are integrated using a singular value decomposition (SVD) inversion technique. The SBAS relies on the use of multiple subsets of images having small baseline via a combination of all the available interferograms constructed from a pair of those subsets (Bhattacharya et al. 2014). The concept behind SBAS is to combine interferograms with a short spatial baseline, in order to minimize the spatial decorrelation (Lauknes et al. 2010).

The basis of the interferometry method is based on the phase difference between the two images of a region, which means that the amplitudes of the waves of two images are multiplied. In fact, the main objective of interferometry is to extract the phase-displacement rate by eliminating or diminishing the effect of other components. The first modification was interferometric phase filtering prior to phase unwrapping. For this, the standard Goldstein filter had been used to reduce decorrelation noise before phase unwrapping. The Goldstein filter is an adaptive filter that is commonly used to reduce the noise contributions from the interferogram (Vajedian et al. 2015).

To provide the piezometric footprint map, monthly records of each piezometric well were considered, and then, using the Mann Kendall test method, each well lowering trend was calculated for 2014–2019. Mann–Kendall method is widely used to evaluate trends in agro-meteorological and hydrological time series. In the Mann–Kendall trend test, the correlation between the rank order of the observed values and their order in time is considered. Piezometrers data were produced by Semnan regional water company. Then, using the kriging method, the mean annual lowering velocity map of water table was obtained. Landsat imagery was used to evaluate built-up land use changes. For this purpose, Landsat images of 1986 and 2017 from study area were classified using the maximum likelihood method. Land use regards anthropogenic activities and natural mechanisms (Nazari et al. 2010), which would modify soil texture and spark subsidence, e.g., mineral extraction, groundwater regime changes, triggering dissolution features (Nadiri et al. 2018a, b).

4 Results and discussion

4.1 InSAR outcome and underground water

The coherency in the studied area was sufficient for InSAR surveying due to aridity and low vegetation density. As shown in Fig. 3, the center of subsidence zone in the Semnan plain with a rate of more than 10 cm per year is located near the railway lines in eastern Semnan. The affected length of the railway is 10 km. However, these land deformation features are spatially correlated with features associated with agricultural development and groundwater extraction in Semnan.

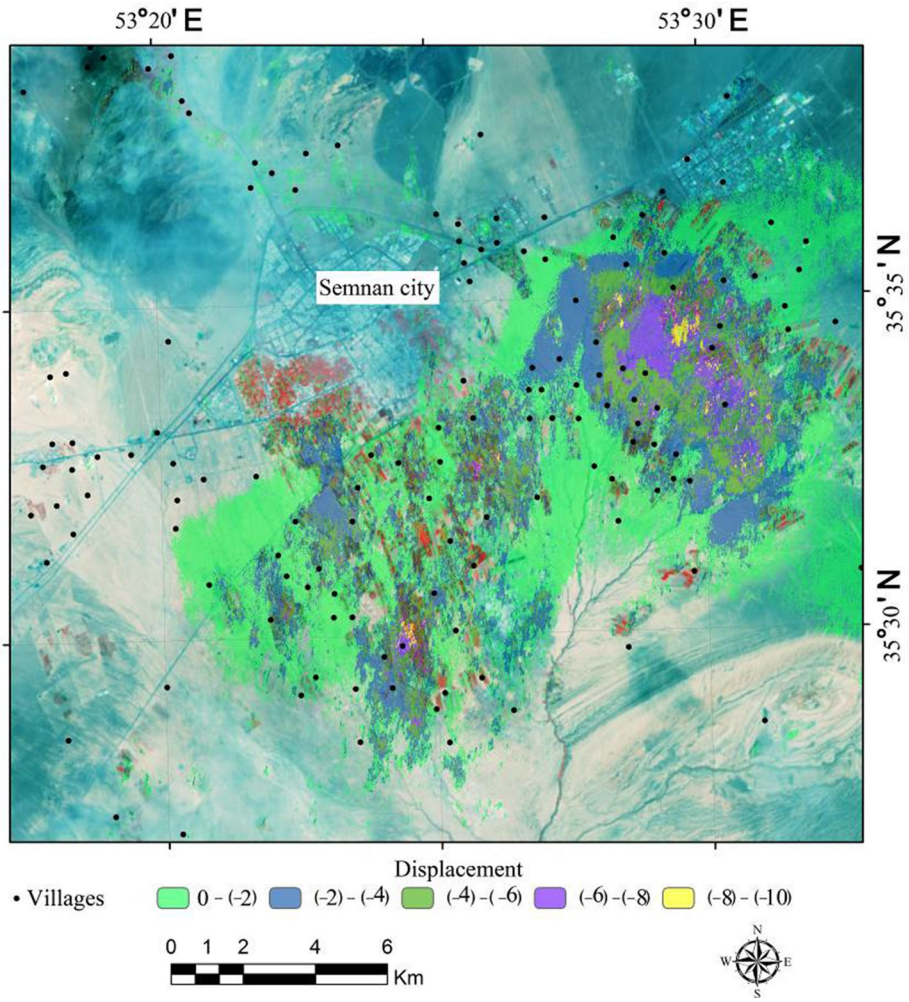

Fig. 3 Annual land displacement rate in Semnan inferred from Sentinel-1A InSAR maximum rate of subsidence in the area is located about 8 km east of Semnan city

By analyzing Fig. 3 it can be retrieved several interesting results. As it is shown in Fig. 4, there are two underground water loss zones. The most important zone is located between industrial town and Semnan city in the east of Semnan city. The second and minor zone is located in western Semnan over gypsiferous and conglomerate formations. Interestingly, the subsided lands are observed in the first zone which is geologically located in clay flat and low level pediment pan foundation (Fig. 5) Which is potentially high compressible. It has been discovered before that the ground surface subsidence is chiefly influenced by the presence of the clays zones (Budhu and Adiyaman 2012). In addition, the proximity of the subsided zone to the industrial town can be regarded as an implication of extreme water pumping for industries. Of course, it should not be neglected that unsustainable irrigated agriculture which is strictly dependent on groundwater has caused tremendous pressure on water resources in this arid area. Also, utilizing the Landsat images obtained in

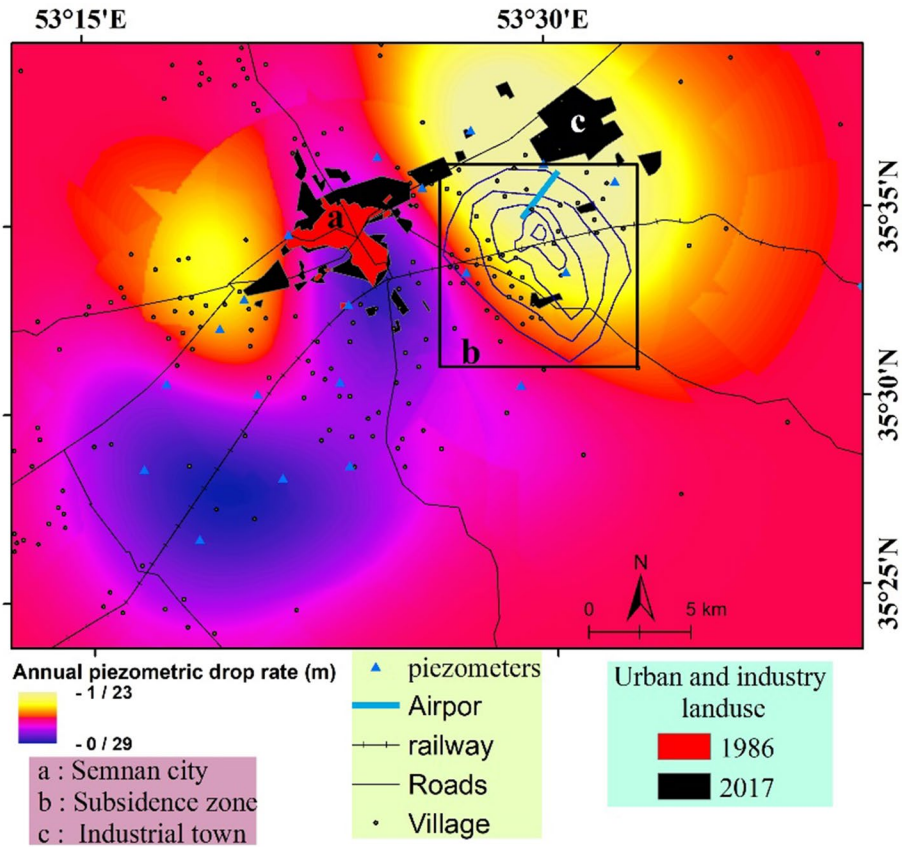

Fig. 4 The mean annual declination rate of piezometric data over the last 10 years (2000–2017) along with subsided area and built-up areas changes between 1986 and 2017 extracted from Landsat. (The contour lines within rectangle of b represent deformed zone obtained by InSAR processing. The outermost and the innermost contour lines exhibit 2 cm/year and 10 cm/year, respectively.)

1986 and 2017 and image classification by the maximum likelihood method, it was noticed that urban and industrial landuse were increased more than four fold over the past 30 years (950 ha in 1986–3900 ha in 2017).

There are also multiple transverse profiles of land subsidence, the rate of groundwater level changes, and the elevation from the sea level in the east–west direction corresponding to the railway line (*MN*) and the north–south axis perpendicular to the railway line (*XZ*) (Figs. 5, 6). As depicted in *MN* profile, it is clear that 15 km of the railroad is located in the subsided zone, and in maximum rate it reaches more than 10 cm per year. According to the *MN* profiles plot, the surface deformation behavior and groundwater drainage show a good spatial relation. In the *XZ* profiles plot, the overall subsidence pattern is spatially correlated with elevation.

The Sentinel-derived subsidence zone spatially agree well with the underground water overexploitation and proximity to growing built-up lands. This confirms the strong inter-twined spatial relation between land deformation, groundwater recharge and landuse changes. It is witnessed numerous examples of finding same pattern by many Iranian

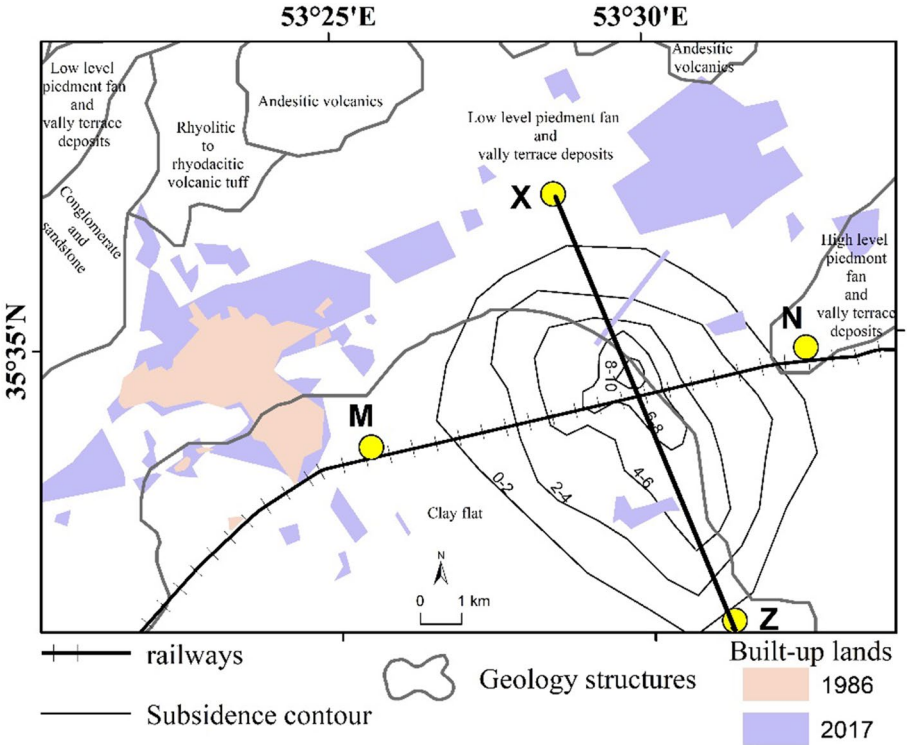

Fig. 5 Geology map of studied area and built-up lands change (including urban and industry landuse) along with displacement velocity contours

researchers. For example, Dehghani et al. (2007) using Envisat discovered the high correlation between the piezometric information and the surface deformation in Mashhad valley (northeast of Iran). Motagh et al (2017) via Alos and Sentinel-1A processing documented that in Rafsanjan plain (located in arid region of Kerman-Iran), there is 30 cm/year subsidence due to intensive groundwater discharge that follows the behavior of Quaternary faults in this area. And Ghazifard et al (2017) also mentioned the deep correlation between formation of earth fissures resulted from subsidence and groundwater head declination and fine-grained sediments in Isfahan (Central Iran). In addition, amplifying subsidence by landuse changes is proved before in many studies (Zhou et al. 2017; Minderhoud et al. 2018).

4.2 Seismicity

Spatial and temporal connection between extreme pumping of groundwater and seismic activities was documented in many papers (Othman et al. 2018; Duda 2016). Figure 7 shows the spatial distribution of earthquake epicenters in 2012–2018. Seismic records was prepared by Iranian Seismological Center. Many earthquake epicenters are close to the subsided zone; their magnitude is more than 1.8 Mn (Fig. 7). The monthly distribution of these records shows that seismic events in Semnan was more frequent in July and August (Fig. 8). Meanwhile, climatic data also indicated that the most environmental dryness due to the region's climate occurs in these 2 months (Fig. 9). With regard to the strong

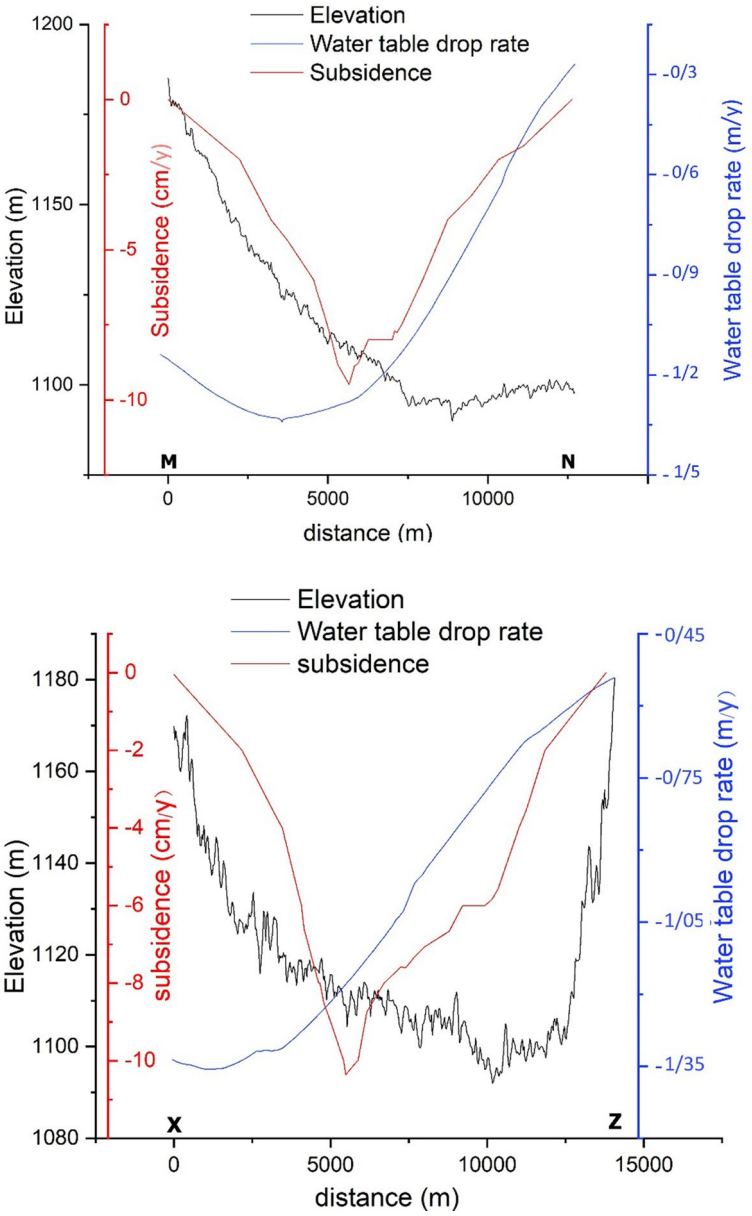

Fig. 6 Multiple linear profiles of InSAR-derived deformation, water table drop rate and elevation along railway line (*M* to *N*) and crossing the railway line (*X* to *Z*) as shown in Fig. 5

dependence on groundwater resources in Semnan, pressure on groundwater resources appears to be higher in these 2 months than in other days. All of this evidence suggests an apparent relation between drought and severe dependence on groundwater resources and seismic activities. Of course, the mechanism of the effect of these phenomena is still unknown to us and requires further research.

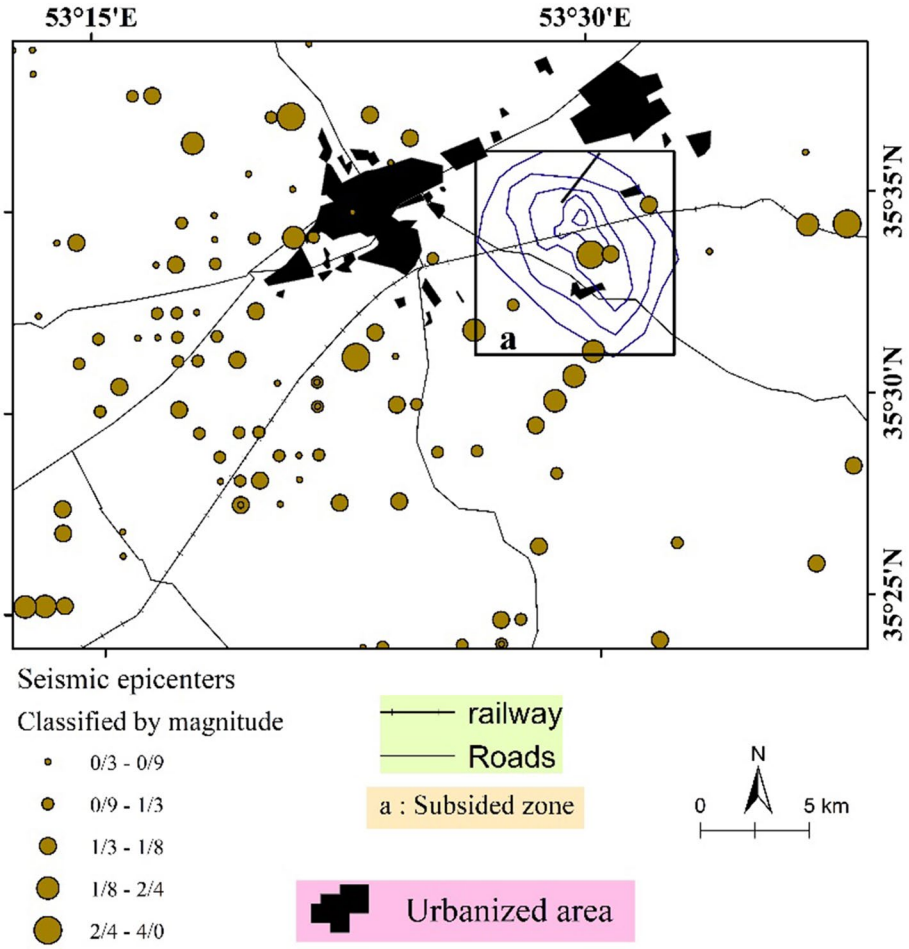

Fig. 7 Spatial distribution of seismic epicenters in study area over last 7 years (2012–2018)

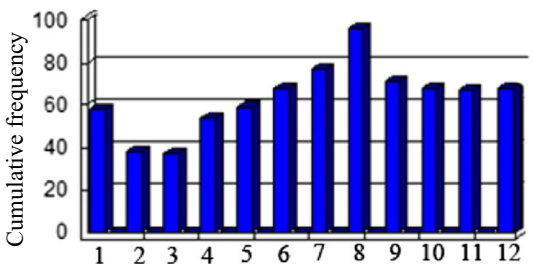

Fig. 8 In study area over last 7 years (2012–2018)

5 Conclusion

The present paper is an attempt to investigate land subsidence hot spots and some triggering factors in Semnan city—central Iran. This study may help to manage side effects

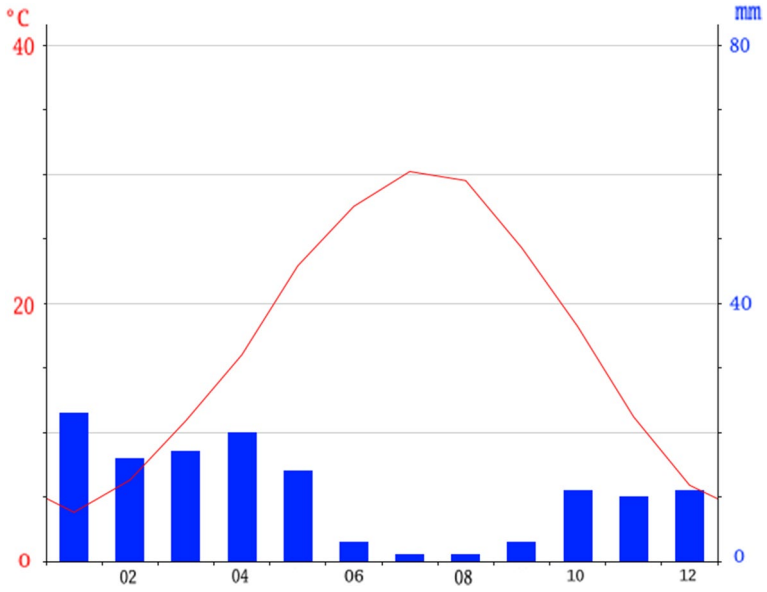

Fig. 9 Mean monthly precipitation (mm) and air temperature (°C) in Semnan (https://en.climate-data.org)

of land subsidence, remediation and recovery of the impacted land. The results of this research illustrated that although the most globally water consumption is in the agricultural land and the industry sector is ranked second (Doungmanee 2016), but due to the concentrated and intense harvesting of underground water in industrial and urban settlements, it may lead to more damage to groundwater resources.

The findings achieved by integrating radar-derived displacement map and geohydrological, landuse and geologic data processing upgrade our knowledge of the mechanisms governing this phenomenon, which could be utilized in the future studies for regulating groundwater withdrawal policies that inhibit or abate its unfavorable effects on populated arid areas. The rapid development of cities has led to large changes in land use patterns around cities, which in developing countries, due to high growth rates, has lead to large changes in land use (Bidgoli et al. 2018). The railway, with its insufficient drainage channels, may acted as a linear barrier that prevents surface water from moving into the desert. Therefore, it causes water accumulation on its north side, which results in earth fissures (Nikbakhti et al. 2018). Some emergency solutions are necessary to avoid unfortunate event inside subsided zone near the railway and the airport. For example, some research recommended that lime and cement injection in soil has significant impact on decreasing the collapsing potential of the soil (Ziaie Moayed and Kamalzare 2015). From the above discussions, it is therefore clear that rapid urbanization accompanied by the considerable increase in built-up area has substantially caused severe pressure on groundwater resources specially in arid environments. For proper water consumption, smart volumetric water metering with blocking capability and overconsumption water tariffs must be established. While a sustainable strategy is pivotal to restoring the water balance in aquifers, any development issues and policies should address subsidence impacts (Nadiri et al. 2018a, b). It is concluded that InSAR continuous monitoring of risky plains is considered as one of the most cost-time effective

methods for identifying the reaction behavior of the plains in association with water management plans.

Acknowledgements The wok was supported by Iran National Science Foundation, Vice-Presidency for science and technology (Grant Number: 96016471). Seismic records was prepared by Iranian Seismological Center. Piezometrers data were produced by Semnan regional water company. We also thank the European Space Agency for free access to Sentinel-1A images (all images are downloaded from "https://vertex.daac.asf.alaska.edu").

References

Angourani S, Memarian H, Shariat Panahi M et al (2014) Dynamic modeling of subsidence in Tehran Plain. Earth Sci 97:211–220

Antonellini M, Giambastiani BMS, Bonzi L et al (2019) Processes governing natural land subsidence in the shallow coastal aquifer of the Ravenna coast, Italy. CATENA 172:76–86

Bell FG (1999) Geological hazards. Their assessment, avoidance and mitigation. Department of Geology and Applied Geology, University of Natal, Durban

Bell JW, Amelung F, Ramelli AR et al (2002) Land subsidence in Las Vegas, Nevada, 1935–2000: new geodetic data show evolution, revised spatial patterns, and reduced rates. Environ Eng Geosci 8(3):155–174

Bhattacharya A, Arora MK, Sharma ML, Vöge M, Bhasin R (2014) Surface displacement estimation using space-borne SAR interferometry in a small portion along Himalayan Frontal Fault. Opt Lasers Eng 53:164–178

Bidgoli RD, Koohbanani H, Yazdani M (2018) Investigation on ecosystem degradation induced by LU/LC changes using landscape pattern indices analysis. Arab J Geosci 11:443. https://doi.org/10.1007/s12517-018-3798-6

Budhu M, Adiyaman I (2012) The influence of clay zones on land subsidence from groundwater pumping. Groundwater 51(1):51–57

Chaussard E, Amelung F, Abidin H, Hong S-H (2013) Sinking cities in Indonesia: ALOS PALSAR detects rapid subsidence due to groundwater and gas extraction. Remote Sens Environ 128:150–161

Chen Y, Zhang K, Tan K, Feng X et al (2018) Long-term subsidence in lava fields at Piton de la Fournaise volcano measured by InSAR: new insights for interpretation of the eastern flank motion. Remote Sens 10:597

Davoodijam M, Motagh M, Momeni M (2015) Land subsidence in Mahyar Plain, Central Iran, investigated using Envisat SAR Data. In: Proceedings the 1st international workshop on the quality of geodetic observation and monitoring systems (QuGOMS'11). Springer, pp 127–130. https://doi.org/10.1007/978-3-319-10828-5_18

Declercq P, Gerard P, Pirard E et al (2017) Subsidence related to groundwater pumping for breweries in Merchtem area (Belgium), highlighted by persistent scaterrer interferometry. Int J Appl Earth Obs Geoinf 63:178–185

Dehghani M (2016) Presentation of a new algorithm based on radar interference technique for monitoring ground level subsidence due to groundwater extraction. Eng Inf Technol 2(2):61–73

Dehghani M, Iliev R, Kaufmann S (2007) Effects of fact mutability in the interpretation of counterfactuals. In: Macnamara DS, Trafton JG (eds) Proceedings of the 29th annual conference of the cognitive science society. Cognitive Science Society, Austin, TX, pp 941–946

Doungmanee P (2016) The nexus of agricultural water use and economic development level. Kasetsart J Soc Sci 37:38–45

Duda J (2016) Relation between benchmark displacement velocity and seismic activity caused by underground longwall exploitation. Acta Geod Geophys 51:709. https://doi.org/10.1007/s40328-015-0154-0

Figueroa-Miranda S, Vargas JT, Ramos-Leal JA et al (2018) Land subsidence by groundwater over-exploitation from aquifers in tectonic valleys of Central Mexico: a review. Eng Geol 246:91–106

Foroughnia F, Nemati S, Maghsoudi Y et al (2019) An iterative PS-InSAR method for the analysis of large spatio-temporal baseline data stacks for land subsidence estimation. Int J Appl Earth Obs Geoinf 74:248–258

Ghazifard A, Akbari E, Shirani K et al (2017) Evaluating land subsidence by field survey and D-InSAR technique in Damaneh city, Iran. Arid Land 9(5):778–789

Haghighatmehr P, Valdanzoj M, Tajik R et al (2011) Analysis of time series of Hashtgert subsidence using radar interferometry method and global positioning system. J Earth Sci 85:105–114
Haghshenas Haghighi M, Motagh M (2019) Ground surface response to continuous compaction of aquifer system in Tehran, Iran: results from a long-term multi-sensor InSAR analysis. Remote Sens Environ 221:534–550
Hejazizadeh Z, Hosseini SM, Karbalaee Dorei A (2015) The simulation of climate change in Semnan province with scenarios of atmospheric general circulation model (Hadcm3). Geogr Environ Hazards 4(15):1–24. https://doi.org/10.22067/geo.v4i3.44214
Hoffmann J (2005) The future of satellite remote sensing in hydrogeology. Hydrogeol J 13:247–250
Holzer TL, Galloway DL (2005) Impacts of land subsidence caused by withdrawal of underground fluids in the United States. Geological Society of America. Rev Eng Geol 16:87–99
Huang Q, Crosetto M, Monserrat O et al (2017) Displacement monitoring and modelling of a high-speed railway bridge using C-band Sentinel-1 data. J Photogramm Remote Sens 128:204–211
Jeanne P, Farr T, Rutqvist J et al (2018) Role of agricultural activity on land subsidence in the San Joaquin Valley, California. Hydrology 569:462–469
Lauknes TR, Piyush Shanker A, Dehls JF, Zebker HA, Henderson IHC, Larsen Y (2010) Detailed rock slide mapping in northern Norway with small baseline and persistent scatterer interferometric SAR time series methods. Remote Sens Environ 114(9):2097–2109
Marbouti M, Praks J, Antropov OE et al (2017) A study of landfast ice with Sentinel-1 repeat-pass interferometry over the Baltic Sea. Remote Sens 9:833
Minderhoud PSJ, Coumu L, Erban LE et al (2018) The relation between land use and subsidence in the Vietnamese Mekong delta. Sci Total Environ 634:715–726
Motagh M, Shamshiri R, Haghshenas Haghighi M et al (2017) Quantifying groundwater exploitation induced subsidence in the Rafsanjan plain, southeastern Iran, using InSAR time-series and in situ measurements. Eng Geol 218:134–151
Nadiri AA, Taheri Z, Khatibi R (2018a) Introducing a new framework for mapping subsidence vulnerability indices (SVIs): ALPRIFT. Sci Total Environ 628–629:1043–1057
Nadiri A, Taheri Z, Kharibi R et al (2018b) Introducing a new framework for mapping subsidence vulnerability indices (SVIs): ALPRIFT. Sci Total Environ 628–629:1043
Nazari SA, Ghorbani M, Kohbanani HR (2010) Landuse changes in Taleghan watershed from 1987 to 2001. Rangeland 4(3):442–451
Nikbakhti O, Hashemi M, Banikheir M et al (2018) Geoenvironmental assessment of the formation and expansion of earth fissures as geological hazards along the route of the Haram-to-Haram Highway, Iran. Bull Eng Geol Environ 77(4):1421–1438
Osmanoglu B, Dixon TH, Wdowinski S et al (2011) Mexico City subsidence observed with persistent scatterer InSAR. Int J Appl Earth Obs Geoinf 13:1–12
Othman A, Sultan M, Becker R et al (2018) Use of geophysical and remote sensing data for assessment of aquifer depletion and related land deformation. Surv Geophys 39:543–566
Ouyang C, Zhao W, An H et al (2019) Early identification and dynamic processes of ridge-top rockslides: implications from the Su Village landslide in Suichang County, Zhejiang Province, China. Landslides 16:799–813
Pirouzi A, Eslami A (2017) Ground subsidence in plains around Tehran: site survey, records compilation and analysis. Geo-Engineering 8(30):1–21
Rodolfo KS, Siringan FP (2006) Global sea-level rise is recognised, but flooding from anthropogenic land subsidence is ignored around northern Manila Bay, Philippines. Disasters 30(1):118–139
Rucci A, Ferretti A, Monti Guarnieri A et al (2012) Sentinel 1 SAR interferometry applications: the outlook for sub millimeter measurements. Remote Sens Environ 120:156–163
Salehi R, Ghafouri M, Lashkaripoor Gh et al (2012) Determination of subsidence of South Mahyar plain using radar interferometry. Water Eng Irrig 3(11):47–57
Samsonov SV, D'Oreye N, González PJ et al (2014) Rapidly accelerating subsidence in the Greater Vancouver region from two decades of ERS-ENVISAT-RADARSAT-2 DInSAR measurements. Remote Sens Environ 143:180–191
Tomas R, Marquez Y, Lopez-Sanchez JM et al (2005) Mapping ground subsidence induced by aquifer overexploitation using advanced differential SAR interferometry: Vega Media of the Segura River (SE Spain) case study. Remote Sens Environ 98:269–283
Tomas R, Herrera C, Lopez-Sanchez JM et al (2010) Study of the land subsidence in Orihuela City (SE Spain) using PSI data: distribution, evolution and correlation with conditioning and triggering factors. Eng Geol 115:105–121

Tung H, Chen H-Y, Hu J-C, Ching K-E, Chen H, Yang K-H (2016) Transient deformation induced by groundwater change in Taipei metropolitan area revealed by high resolution X-band SAR interferometry. Tectonophysics 692:265–277

Vajedian S, Serajiyan MR, Mansouri A (2010) Extraction of 3D displacement field by using SAR (case study of Bam Fault). Phys Time Space 37(2):83–96

Vajedian S, Motagh M, Nilfouroushan F (2015) StaMPS improvement for deformation analysis in mountainous regions: implications for the Damavand volcano and Mosha fault in Alborz. Remote Sens 7(7):8323–8347

Zerbini S, Richter B, Rocca F, van Dam T, Matonti F (2007) A combination of space andterrestrial geodetic techniques to monitor land subsidence: case study, the South-eastern Po Plain, Italy. J Geophys Res Solid Earth 112(B5):B05401

Zhou C, Gong H, Chen B et al (2017) InSAR time-series analysis of land subsidence under different land use types in the eastern Beijing plain, China. Remote Sens 9:380

Ziaie Moayed R, Kamalzare M (2015) Improving physical characteristics of collapsible soil (case study: Tehran–Semnan railroad). Eng Geol 9(2):2869–2890